

# On the Interfacial Width in Triblock versus Diblock Copolymers: A Neutron Reflectivity Investigation

S. H. Anastasiadis\*,† and H. Retsos†

Foundation for Research and Technology–Hellas, Institute of Electronic Structure and Laser,  
P.O. Box 1527, Heraklion Crete, Greece

C. Toprakcioglu‡

University of Patras, Physics Department, 265 00 Rio Patras, Greece

A. Menelle

Laboratoire Léon Brillouin (CEA-CNRS), C.E.N. Saclay, 91391 Gif-Sur-Yvette Cedex, France

G. Hadziioannou

Groningen University, Chemistry Department and Materials Science Center,  
9747 AG Groningen, The Netherlands

Received April 7, 1998; Revised Manuscript Received June 28, 1998

**ABSTRACT:** The relationship between the interfacial width in a lamellar triblock copolymer and that in the respective lamellar diblock has been investigated by neutron reflectivity, taking advantage of the surface-induced orientation of the domains parallel to the free surface in thin copolymer films. The effective interfacial width in a poly(vinyl-2-pyridine)–polystyrene–poly(vinyl-2-pyridine) triblock is found to be ~38% narrower than that for the respective diblock. This difference is discussed in relation to theoretical predictions and is tentatively attributed to a reduced contribution of the thermal fluctuations of the concentration profiles to the effective interfacial width because of the presence of the mid-block bridges connecting the end-block domains in the triblock lamellae.

## Introduction

The surface-induced orientation of the lamellar domains in ordered diblock copolymers<sup>1,2</sup> has provided a direct, convenient way to investigate the interfacial widths<sup>2</sup> between the adjacent microdomains by using neutron reflectivity<sup>1,2</sup> (NR), which allows the study of interfaces with precision of  $<10$  Å. The effective interfacial widths for symmetric polystyrene–poly(methyl methacrylate) (PS–PMMA) diblocks were found<sup>2</sup> to be  $50 \pm 5$  Å, independent of the diblock molecular weight (MW) in the range 30 000 to 300 000. Moreover, the effective widths of the interfaces between the microphases in ordered PS–PMMA diblocks were demonstrated to be identical<sup>2</sup> to those between the respective homopolymers, PS and PMMA, although, intuitively, one may have expected that the entropic cost due to the localization of the junction points near the diblock interface would influence the interfacial widths relative to that between homopolymers. Subsequent theories<sup>3–5</sup> addressed this behavior by accounting for both the effects of the finite MWs as well as the contribution of the thermal fluctuations of the composition profiles<sup>5</sup> (or the capillary waves<sup>4</sup> at the interface) to the measured effective interfacial widths. Semenov suggested<sup>5</sup> that the inherent interface in diblocks differed from that between the respective homopolymers, but that the increased contribution of the interfacial fluctuation corrections in homopolymer bilayers led to the similarity of the measured effective interfacial

widths; this theory<sup>5</sup> agrees very well with the data<sup>2</sup> for PS–PMMA.

For A–B–A triblock copolymers, two junction points per chain are localized at the respective interfaces, which may lead to a broadening of the inherent interface, whereas the bridge configuration of the middle block connecting two opposing interfaces may affect the interfacial fluctuations. It is, therefore, tempting to investigate the relation between the interfacial widths in triblock versus diblock copolymers. To our knowledge, there is only one NR study<sup>6</sup> on surface-oriented symmetric poly(vinyl-2-pyridine)–polystyrene–poly(vinyl-2-pyridine) triblocks, where an interfacial width of  $38 \pm 3$  Å was reported; this work will also be discussed below.

In this paper, we present a NR study of the behavior of thin films of symmetric diblock and triblock copolymers of deuterated polystyrene (PS) and poly(vinyl-2-pyridine) (PV2P) on Si wafers, aiming at investigating the relationship between the interfacial widths in the two systems. The perfect orientation of the lamellar domains of a PV2P–PS–PV2P triblock parallel to the surface allowed us to evaluate the effective interfacial width ( $28 \pm 3$  Å), which is ~38% narrower than that of the respective PS–PV2P diblock ( $45 \pm 3$  Å). The measured effective interfacial widths are discussed in relation to theory<sup>3–5</sup> and to other measurements of the PS–PV2P system.<sup>6–9</sup> Different contributions of the interfacial fluctuation corrections in triblocks, attributable to the bridging mid-block chains, are probably responsible for the observed effect dominating over differences in the entropic cost of localization of two junction points at the interfacial region in the triblocks.

\* To whom correspondence should be addressed.

† Also at University of Crete, Physics Department, 710 03 Heraklion Crete, Greece.

‡ Also at Foundation for Research and Technology–Hellas.

**Table 1. Molecular Characteristics of the Copolymers**

Sample	$M_n$	$M_w$	$M_w/M_n$	wt % PS	$N^a$	$f_{PS}^b$
PS-PV2P 60-60	100 000	108 000	1.08	50	996	0.465
PV2P-PS-PV2P 30-60-30	95 400	103 000	1.08	50	950	0.465

<sup>a</sup> Weight average degree of polymerization. <sup>b</sup> Polystyrene volume fraction.

## Experimental Section

PS-PV2P diblock and PV2P-PS-PV2P triblock copolymers were synthesized by anionic polymerization under inert gas in tetrahydrofuran at  $-70^\circ\text{C}$ , with monomers added sequentially (the styrene monomers were perdeuterated); their molecular characteristics are shown in Table 1 (the same copolymers were used previously<sup>6,7</sup>). Thin copolymer films were prepared by spin-coating the polymers from toluene solutions onto polished Si disks (5 cm in diameter, 5 mm thick) that were subsequently placed at  $60^\circ\text{C}$  under vacuum to remove the remaining solvent, annealed for 24 h at  $170^\circ\text{C}$  to reach equilibrium, and then rapidly quenched to room temperature. The NR measurements were performed at room temperature.

The NR experiments were performed with the time-of-flight DESIR reflectometer at the ORPHEE reactor (Laboratory Léon Brillouin); instrument details are given elsewhere.<sup>10</sup> In brief, a collimated ( $\sim 0.01$ – $0.03^\circ$ ) neutron beam with a distribution of wavelengths  $4 < \lambda < 18 \text{ \AA}$  impinged upon the specimen surface at a fixed angle,  $\theta$ . Variation in the range of the component of the incident neutron momentum perpendicular to the film surface,  $k_0 = (2\pi/\lambda) \sin \theta$ , is achieved via rotation of the sample with respect to the incident beam (varying  $\theta$ ); for the highest  $\theta$  ( $3.5^\circ$ ), the  $k_0$  range extends to  $\sim 0.08 \text{ \AA}^{-1}$  with the corresponding reflectivities  $R$  extending down to  $10^{-4}$ – $10^{-5}$ . The principles of NR have been discussed previously<sup>1,2</sup> and are not reproduced here. We note only that the instrumental resolution in  $k_0$  space is  $\delta k_0/k_0 \approx \delta\theta/\theta + \delta\lambda/\lambda$  and, for fixed incident collimation ( $\delta\theta$ ) and wavelength detection ( $\delta\lambda$ ), the reflectivities measured at different values of  $\theta$  contain different resolution functions and cannot be superimposed. The resolution function at each  $\theta$ , assumed to have Gaussian distribution with a full-width at half-maximum of  $\delta k_0$ , is convoluted with the calculated reflectivity profiles and then compared with the experimental reflectivity curves.

## Results and Discussion

Figure 1 shows the NR data for a film  $\sim 1900 \text{ \AA}$  thick of the symmetric PS-PV2P 60-60 diblock as reflectivity  $R$  vs  $k_0$ . The two different sets of data, displaced by two orders of magnitude for clarity, represent measurements at incident angles of  $0.5^\circ$  and  $2.0^\circ$ . The  $k_0$  range at  $\theta = 0.5^\circ$  extends below the critical angle, allowing normalization of the  $R$  axis by setting to 1 the constant value for a range of small  $k_0$  values; the  $R$  axis for the  $\theta = 2.0^\circ$  data is scaled to that for  $\theta = 0.5^\circ$  in featureless regions of the reflectivity curve. Six orders of Bragg reflections are observed because of the orientation of the lamellae parallel to the film-free surface, i.e., a multilayered structure of alternating PV2P and PS domains; cross-sectional imaging<sup>11</sup> of thin diblock films by transmission electron microscopy showed the predominant domain orientation parallel to the surface. This behavior agrees with studies of symmetric PS-PMMA,<sup>1,2</sup> PS-PV2P,<sup>7-9,12</sup> and polyolefin<sup>13</sup> thin diblock films as well as with the predictions<sup>4,14</sup> of theory and computer simulations.

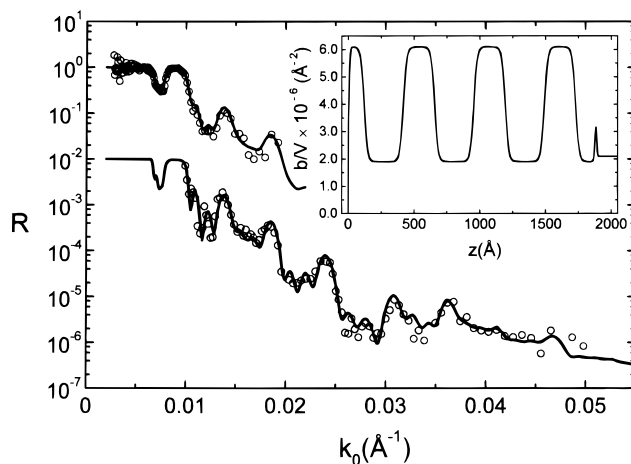


**Figure 1.** Experimental NR profile (circles) as a function of  $k_0$  for a thin film of the PS-PV2P 60-60 diblock (the styrene units are deuterated) annealed for 24 h at  $170^\circ\text{C}$ . The two different sets of data, measured at  $0.5^\circ$  and  $2.0^\circ$  angles of incidence, have been offset by factors 1 and  $10^{-2}$  for clarity. The solid lines represent the calculated reflectivity curves obtained by using the scattering length density profile shown in the inset (zero corresponds to the air/polymer surface).

The solid lines in Figure 1 are the calculated reflectivity curves, convoluted with the appropriate resolution functions for the two  $\theta$ s, obtained by using the scattering length density profile in the inset ( $z = 0$  denotes the air/polymer surface). The multilayered structure is composed of 3.5 periods, with the lower-surface-energy PS located at the air/polymer surface and the PV2P being at the polymer/Si (or  $\text{SiO}_2$ ,  $\sim 12 \text{ \AA}$ ) interface. As with PS-PMMA<sup>2</sup> and with recent work on PS-PV2P,<sup>8,9</sup> the analysis did not require adjusting the thicknesses of the layers adjacent to the air/polymer and polymer/substrate interfaces to be any different from exactly one-half of the respective layers of the underlying multilayered structure—in disagreement with an earlier investigation on the same copolymer.<sup>7</sup> The earlier discussion<sup>7</sup> was based on the difference between the total thickness estimated from X-ray reflectivity and  $(m + 1/2)L$ , with  $m$  being an integer and  $L$  the copolymer long-period; however, the presence of relief island or hole domains<sup>15</sup> on the free surface of the film is well-known to take care of the difference between the apparent total thickness and the actual multilayered morphology. The parameters obtained by the best-fit to the data are shown in Table 2. The value obtained,  $L = L_{PS} + L_{PV2P} \approx 536 \text{ \AA}$ , agrees very well with results from earlier studies of PS-PV2P diblocks.<sup>16</sup>

Within the precision of the data and the analysis, and assuming a hyperbolic tangent functional form of the interfacial profile, the effective interfacial thickness between the PS and PV2P microdomains in the ordered diblock is estimated to be  $a_I \approx 45 \pm 3 \text{ \AA}$ ; the interfacial width is defined as  $a_I = (\phi^\beta - \phi^\alpha)/(\partial\phi(z)/\partial z)_{\phi=(\phi^\alpha+\phi^\beta)/2}$ , where  $\phi^\alpha$  and  $\phi^\beta$  denote the compositions of the two microphases away from the interface. This value is consistent<sup>17</sup> with those reported by Torikai et al.<sup>8,9</sup> but is 16% broader than the one estimated by de Jeu et al.<sup>7</sup> The best-fit values for the scattering length densities

**Table 2. Characteristics of the Copolymers Measured by NR**

Sample	$L_{PS},^a \text{ \AA}$	$(b/V)_{PS},^b 10^{-6} \text{ \AA}^{-2}$	$L_{PV2P},^a \text{ \AA}$	$(b/V)_{PV2P},^b 10^{-6} \text{ \AA}^{-2}$	$L, \text{ \AA}$	$\sigma_{air},^c \text{ \AA}$	$\sigma_{sub},^d \text{ \AA}$	$a_{I_{exp}}, \text{ \AA}$
PS-PV2P 60-60	$238 \pm 2$	6.1	$298 \pm 2$	1.9	536	6	6	$45 \pm 3$
PV2P-PS-PV2P 30-60-30	$131 \pm 5$	6.1	$164 \pm 4$	1.9	295	4	4	$28 \pm 3$

<sup>a</sup>  $L_J$  is the thickness of the  $J$  microdomain. <sup>b</sup>  $(b/V)_J$  is the scattering length density of the  $J$  microdomain. <sup>c</sup> Root-mean-squared roughness at the air/polymer interface. <sup>d</sup> Root-mean-squared roughness at the copolymer/substrate interface. A thin  $\text{SiO}_2$  layer is used on top of the Si wafer: 12 Å for the diblock and 18 Å for the triblock.

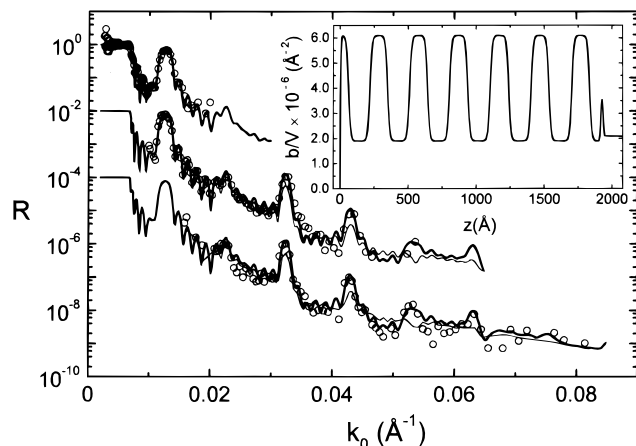


**Figure 2.** Experimental NR profile (circles) as a function of  $k_0$  for a thin film of the PV2P-PS-PV2P 30-60-30 triblock (the styrene units are deuterated) annealed for 24 h at 170 °C. The three different sets of data, measured at 0.5°, 2.0°, and 3.5° angles of incidence, have been offset by factors 1,  $10^{-2}$ , and  $10^{-4}$ , respectively, for clarity. The heavy solid lines represent the calculated reflectivity curves obtained by using the scattering length density profile shown in the inset (zero corresponds to the air/polymer surface). The thin lines represent the calculated reflectivity curves obtained by using the interfacial width estimated from the diblock data in Figure 1.

$(b/V)$  for the two microphases indicate almost pure microphases, in agreement with the former authors,<sup>8,9</sup> but in disagreement with the latter<sup>7</sup>; since the diblock is well within the strong segregation limit (SSL), as will be discussed below, pure microphases are expected.

Figure 2 shows the NR data for a film ~2000 Å thick of the symmetric PV2P-PS-PV2P 30-60-30 triblock. The three different sets of data, displaced by two decades from each other, represent measurements performed at incident angles of 0.5°, 2.0°, and 3.5°. The  $R$ -axis was normalized as described for the diblock film. Six orders of Bragg reflections were observed, indicating the orientation of the lamellae parallel to the free surface; interference optical microscopy on annealed thin triblock films<sup>18</sup> shows a quantization of the film thickness due to the alignment of the microdomains with the presence of islands or holes if the total film thickness is different from  $(p + 1/2)L$ , where  $p$  is an integer, similar to the results for studies of diblocks.<sup>15</sup> The solid lines are the calculated reflectivity curves, convoluted with the appropriate resolution functions for the three angles and using the scattering length density profile in the inset with a hyperbolic tangent interfacial profile. As in the diblock, PS is attracted to the air surface and PV2P is preferentially located at the substrate interface (note the 18 Å  $\text{SiO}_2$ ), whereas the structure is composed of 6.5 bilayers of PS and PV2P microdomains, with  $b/V$  values almost equal to those for the pure components (Table 2) and with the thicknesses of the top and bottom layers equal to one-half of those of the multilayered structure. The extracted effective interfacial width ( $a_I$ ) is  $\approx 28 \pm 3$  Å, whereas

the roughnesses at the free surface and at the substrate are close to the generally accepted values (4 Å);  $a_I$  is not very close to the value obtained before,<sup>6</sup> probably because of differences in the analysis procedures used and the significantly different values for the roughnesses of the surface and substrate used there.<sup>6</sup>

The value for the effective interfacial width between the microdomains of the triblock copolymer is, therefore, 38% narrower than the value obtained between the microdomains of the diblock. The thin lines in Figure 2 show the calculated reflectivity curves obtained by using the interfacial width of 45 Å measured for the diblock; the unacceptable quality of the fit is especially evident by the loss of features at the high- $k_0$  range. The MWs for the two systems are not the same (the respective diblock for the triblock under investigation would have been a PS-PV2P 30-30); however, the interfacial widths should be independent of the MW in the present range.<sup>2,5</sup> The difference in the values obtained is discussed below.

The ordered state of diblock copolymers has for almost three decades attracted the attention of theoreticians, who have proffered theories addressing the equilibrium diblock structure, i.e., the long-period  $L$  and the interfacial thickness  $a_I$ . Although agreement with the data for the lamellae period is generally very good, the situation regarding the comparison between measured and calculated values of the interfacial thickness is still unclear. The interfacial tension and interfacial thickness between two homopolymers were evaluated<sup>19</sup> within the mean-field theory for infinite MWs in the SSL:

$$\gamma_\infty = k_B T b_K (\chi/6)^{1/2} / v; a_{I_\infty} = 2 b_K (6\chi)^{-1/2} \quad (1)$$

where  $b_K$  is the average Kuhn statistical segment length,  $v$  the average monomeric volume,  $\chi$  the Flory-Huggins interaction parameter, and  $k_B T$  the thermal energy. The narrow-interface-approximation theory<sup>20</sup> mandates that the interface between the domains in a diblock copolymer is identical to that between the respective homopolymers of infinite MWs; Shull and co-workers verified<sup>4</sup> this limiting behavior for infinite incompatibility degrees ( $\chi N$ s).

The finite-MW effects on the interfacial properties between homopolymers were introduced<sup>21</sup> later, leading to a decrease in the interfacial tension and an increase in interfacial thickness compared with the values at infinite MWs, because of chain-end effects; however, even those predictions failed to quantitatively account for the measured effective interfacial widths.<sup>2</sup> Semenov<sup>5</sup> analytically evaluated the correction to the interfacial width attributable to the polymer-end effects, specifically for diblocks in the SSL:

$$a_{I_N} = a_{I_\infty} [1 + 2L(\chi N)^{-1}] \approx a_{I_\infty} [1 + 1.34(\chi N)^{-1/3}] \quad (2)$$

where  $a_{I_\infty}$  is as defined by eq 1; this correction is much stronger for diblocks than for polymer blends<sup>21</sup> because



**Table 3. Comparison between Experimental and Theoretical Interfacial Widths**

Sample	$N$	$N_{\text{eff}}^a$	$L, \text{\AA}$	$\chi N_{\text{eff}}$	$a_{I_\infty},^b \text{\AA}$	$a_{I_N},^c \text{\AA}$	$a_{I_{\text{eff}}},^d \text{\AA}$	$a_{I_{\text{exp}}}, \text{\AA}$
PS-PV2P 60-60	996	996	536	108.6	17.6	22.6	33.6	$45 \pm 3$
PV2P-PS-PV2P 30-60-30	950	475	295	51.8	17.6	24.1	33.0	$28 \pm 3$

<sup>a</sup> For the triblock  $N_{\text{eff}} = N/2$ . <sup>b</sup> Calculated with eq 1. <sup>c</sup> Calculated with eq 2. <sup>d</sup> Calculated with eq 3 and using the experimental value of  $L$ .

of the connectivity of the blocks. Moreover, Shull and co-workers<sup>4</sup> and Semenov<sup>5</sup> have discussed the contribution of the fluctuations in the position of the interface to the measured effective interfacial widths, with Shull proposing an expression based on the theories of capillary waves at the liquid/vapor interface. Semenov, however, considered the effects of the thermal fluctuations of the concentration profiles, i.e., the fact that the interface defined by  $\phi = 0.5$  is not located at  $z = 0$  (as in mean-field) but rather defines a rough surface  $z = \zeta(x, y, t)$ , with  $x, y$  being the other coordinates and  $t$  the time. The statistical properties of this surface are governed by the additional contribution to the free energy from the increase of the interfacial area, leading to the calculation of the variance  $s^2 \equiv \langle \zeta^2 \rangle$  of the Gaussian distribution of the surface  $\zeta(x, y, t)$ . The effective interfacial width is, then, modified to

$$a_{I_{\text{eff}}} = \left[ a_{I_N}^2 + \frac{3va_{I_\infty}}{b_K^2} \ln(L/a_{I_\infty}) \right]^{0.5} \quad (3)$$

where  $a_{I_\infty}$  and  $a_{I_N}$  are as given in eqs 1 and 2, respectively.

In Table 3, the data for the effective interfacial widths for the diblock and the triblock are compared with the values estimated by eqs 1–3, with  $\chi = -0.033 + 63/T$  (based on the polymerization degree  $N$ ),<sup>22</sup>  $b_K = 6.8 \text{\AA}$ , and  $v = 95.3 \text{ cm}^3/\text{mol} = 158 \text{\AA}^3/\text{mer}$  (the geometric mean of the monomeric volumes of deuterated PS and PV2P). The incompatibility degrees are  $\chi N_{\text{eff}} \approx 108$  and 52 for the diblock and the triblock, respectively; thus, definitely the diblock but also the triblock can be regarded as within the SSL.

Because no detailed calculation exists on the domain structure and the interface in triblocks, the calculations in Table 3 are presented for the diblock PS-PV2P 30-30. The long-period of a triblock  $A_n B_{2n} A_n$  agrees very well with that of the  $A_n B_n$  diblock,<sup>23</sup> whereas the order-disorder transition for the  $A_n B_{2n} A_n$  occurs at higher values of  $\chi n$  than for the  $A_n B_n$ ; i.e., the presence of two A-B junction points per chain makes the system more compatible.<sup>24</sup> Although one might expect that the increased entropic losses due to the localization of two junction points per chain at the interfacial regions in an ordered triblock should influence the interfacial behavior, the comparison in Table 3 does not take this into account.

The effect of the difference in MW between the diblock and half of the triblock does not substantially affect calculations of the effective interfacial widths in Table 3 (at least for the present range of MWs) and therefore cannot explain the difference between the measured values of the diblock and the triblock.<sup>25</sup> Similarly, from the results of the numerical calculations in Figures 1 and 2 of Melekevitze and Muthukumar,<sup>3</sup> we would predict an insignificant difference for the parameters  $\sigma_0$  that characterize the interface for the two present MWs; the same is true<sup>26</sup> if one uses Figure 4 of Shull<sup>4a</sup> with eq 22 of Shull et al.<sup>4b</sup> Moreover, although the

calculated values appear to be closer to the measured values for the triblock than for the diblock, we suspect this is just fortuitous<sup>25</sup>; the fact that the calculation does not predict any difference between the two systems means that the experimentally observed difference may be the result of different contributions of the interfacial fluctuations term to the effective interfacial widths. The presence of the bridging configuration of the mid-block chains in the triblock (connecting the two opposing end-block domains) should influence the stretching elastic energy,<sup>27</sup> which affects the variance of the interfacial thermal fluctuations; we suggest that the bridges may reduce the variance  $s^2$  and thus lead to a smaller contribution to the measured effective interfacial widths. In a complete theory for the structure of triblocks, one should probably explicitly take into account the localization of the two junction points per chain compared with only one for the respective diblock, which could influence both the intrinsic interfacial width for entropic reasons (localization) and the interfacial fluctuations for chain-stretching reasons; this question is left for the theoreticians.

### Concluding Remarks

In this investigation of the relation between the effective interfacial widths between the microdomains of a diblock versus a triblock copolymer, the orientation of the lamellae parallel to the surface allowed the investigation of the interface with a resolution of  $<5 \text{\AA}$ . The difference in effective widths (the triblock being  $\sim 38\%$  narrower than the respective diblock) could not be accounted for by the small difference in the MWs of the systems investigated and are probably related to the effect of the bridges in the triblock copolymer morphology. Further theoretical investigation of this is needed.

**Acknowledgment.** S.H.A. acknowledges that part of this research was sponsored by NATO's Scientific Affairs Division in the framework of the Science for Stability Program and by the Greek General Secretariat of Research and Technology. The financial support of the European Union in the framework of the Human Capital and Mobility Program is acknowledged by S.H.A. and G.H. (contract CHRX-C.T.93-0370) and by C.T. (contract CHRX-C.T.94-0696). G.H. acknowledges the financial support of The Netherlands Technology Foundation (SON-STW) and The Netherlands Organization for Scientific Research (NWO). We thank Dr. B. Factor and C. Vavakis for their help with the reflectivity experiments.

### References and Notes

- (1) Anastasiadis, S. H.; Russell, T. P.; Satija, S. K.; Majkrzak, C. F. *Phys. Rev. Lett.* **1989**, *62*, 1852.
- (2) Anastasiadis, S. H.; Russell, T. P.; Satija, S. K.; Majkrzak, C. F. *J. Chem. Phys.* **1990**, *92*, 5677.
- (3) Melekevitze, J.; Muthukumar, M. *Macromolecules* **1991**, *24*, 4199.
- (4) (a) Shull, K. R. *Macromolecules* **1992**, *25*, 2122. (b) Shull, K. R.; Mayes, A. M.; Russell, T. P. *Macromolecules* **1993**, *26*, 3929.

- (5) Semenov, A. N. *Macromolecules* **1993**, *26*, 6617.
- (6) de Jeu, W. H.; Lambooy, P.; Hamley, I. W.; Vaknin, D.; Pedersen, J. S.; Kjaer, K.; Seyger, R.; van Hutten, P.; Hadzioannou, G. *J. Phys. II (Paris)* **1993**, *3*, 139.
- (7) de Jeu, W. H.; Lambooy, P.; Vaknin, D. *Macromolecules* **1993**, *26*, 4973.
- (8) Torikai, N.; Noda, I.; Matsushita, Y.; Karim, A.; Satija, S. K.; Han, C. C.; Ebisawa, T. *J. Phys. Soc. Jpn.* **1996**, *65*, 128.
- (9) Torikai, N.; Noda, I.; Karim, A.; Satija, S. K.; Han, C. C.; Matsushita, Y.; Kawakatsu, T. *Macromolecules* **1997**, *30*, 2907.
- (10) Kent, M. S.; Lee, H.-T.; Farnoux, B.; Rondelez, F. *Macromolecules* **1992**, *25*, 6240.
- (11) Esselink, E.; Hadzioannou, G., unpublished data.
- (12) Li, Z.; Qu, S.; Rafailovich, M. H.; Sokolov, J.; Tolan, M.; Turner, M. S.; Wang, J.; Schwarz, S. A.; Lorenz, H.; Kotthaus, J. P. *Macromolecules* **1997**, *30*, 8410.
- (13) Sikka, M.; Singh, N.; Karim, A.; Bates, F. S.; Satija, S. K.; Majkrzak, C. F. *Phys. Rev. Lett.* **1993**, *70*, 307.
- (14) Tang, H.; Freed, K. F. *J. Chem. Phys.* **1992**, *97*, 4496. Binder, K. *Acta Polym.* **1995**, *46*, 2041.
- (15) Coulon, G.; Ausserre, D.; Russell, T. P. *J. Phys. (Paris)* **1990**, *51*, 777. Grim, P. C. M.; Nyrkova, I. A.; Semenov, A. N.; ten Brinke, G.; Hadzioannou, G. *Macromolecules* **1995**, *28*, 7501.
- (16) Matsushita, Y.; Mori, K.; Sagushi, R.; Nakao, Y.; Noda, I.; Nagasawa, M. *Macromolecules* **1990**, *23*, 4313.
- (17) An error-function profile was used<sup>8,9</sup> with the full-width at half-maximum being 45 Å; this equals  $2.355\sigma$  (where  $\sigma$  is the standard deviation), and the interfacial width<sup>2</sup> is  $a_I = \sqrt{2\pi}\sigma = 48$  Å. A conversion error was introduced<sup>9</sup> whereby  $a_I$  was reported to equal 24 Å, probably due to miscalculating the half-width at half-maximum ( $=1.17741\sigma$ ) as the full width at half-maximum. Personal communication to the authors clarified this point.
- (18) Anastasiadis, S. H.; Hadzioannou, G., unpublished data.
- (19) Helfand, E.; Tagami, Y. *J. Chem. Phys.* **1971**, *56*, 3592; **1972**, *57*, 1812.
- (20) Helfand, E.; Wasserman, Z. R. *Macromolecules* **1976**, *9*, 879.
- (21) Anastasiadis, S. H.; Gancarz, I.; Koberstein, J. T. *Macromolecules* **1988**, *21*, 2980. Helfand, E.; Bhattacharjee, S. M.; Fredrickson, G. J. *J. Chem. Phys.* **1989**, *91*, 7200. Broseta, D.; Fredrickson, G. H.; Helfand, E.; Leibler, L. *Macromolecules* **1990**, *23*, 132. Tang, H.; Freed, K. F. *J. Chem. Phys.* **1991**, *94*, 6307. Ermoshkin, A. V.; Semenov, A. N. *Macromolecules* **1996**, *29*, 6294.
- (22) Dai, K. H.; Kramer, E. J. *Polymer* **1994**, *35*, 157.
- (23) Hadzioannou, G.; Skoulios, A. *Macromolecules* **1982**, *15*, 258; **1982**, *15*, 267. Matsushita, Y.; Nomura, M.; Watanabe, J.; Mogi, Y.; Noda, I.; Imai, M. *Macromolecules* **1995**, *28*, 6007. Matsen, M. W.; Schick, M. *Macromolecules* **1994**, *27*, 187. Jones, R. L.; Kane, L.; Spontak, R. J. *Chem. Eng. Sci.* **1996**, *51*, 1365.
- (24) Koberstein, J. T.; Russell, T. P.; Walsh, D. J.; Pottick, L. *Macromolecules* **1990**, *23*, 877. Gehlsen, M. D.; Almdal, K.; Bates, F. S. *Macromolecules* **1992**, *25*, 939. Mayes, A. M.; Olvera de la Cruz, M. *J. Chem. Phys.* **1989**, *91*, 7228.
- (25) If different<sup>9,16</sup>  $\chi$  values are used ( $\chi \approx 0.0724$  at 170 °C), as in Torikai et al.,<sup>9</sup> the predictions for  $a_{I,eff}$  in Table 3 are 37.9 Å for the diblock and 37.6 Å for the triblock. If  $\chi$  is adjusted to 0.0472, the predictions agree perfectly with the measurements for the diblock ( $a_{I,eff} \approx 45.0$  Å), similar to the finding for PS-PMMA,<sup>2,5</sup> and give  $a_{I,eff} \approx 45.4$  Å for the triblock.
- (26) If the lateral coherence length of NR is used as the long-wavelength cutoff ( $\lambda_{max}$ ), the values are 45 and 46 Å for  $a_{I,eff}$  for the diblock and the triblock, respectively, whereas if the period  $L$  is used<sup>5</sup> as  $\lambda_{max}$ , the predictions are 37 Å for both.
- (27) Zhulina, E. B.; Halperin, A. *Macromolecules* **1992**, *25*, 5730.

MA980551Y